Nano-Magnetic Probing on Magnetite (110)

Gabriela Maris[1], Lucian Jdira[1], Jan G. H. Hermsen[1], Shane Murphy[2], Giuseppe Manai[2], Igor V. Shvets[2], and Sylvia Speller[1]

[1]Experimental Solid State Physics II, Institute for Molecules and Materials, Radboud University Nijmegen, 6525 ED Nijmegen, The Netherlands
[2]SFI Nanoscience Laboratory, Department of Physics, Trinity College, Dublin 2, Ireland

We report our results on the structure and magnetic imaging of Fe_3O_4 (110) thin films using scanning tunneling microscopy/spectroscopy (STM/STS). Based on atomically resolved STM images we present a model for the observed ridge reconstruction of the surface, in agreement with a bulk-truncated layer containing both octahedral and tetrahedral iron ions. The weak contrast between the tops and the valleys of the ridges in the current map measured with W tips is attributed to the tetrahedral and octahedral character, respectively. We observe a contrast enhancement at the W tip change accompanied by a corrugation enhancement. An antiferromagnetic MnNi tip detects a large contrast between tops and valleys in the current map and two surprising states, at 0.3-V and −0.7-V bias voltages. We attribute the observed contrast to magnetism in agreement with our proposed model.

Index Terms—**Ferrimagnetic films, ferrite films, magnetic domains, surfaces.**

I. Introduction

SPIN-POLARIZED scanning tunneling microscopy (STM) and spectroscopy (STS) allowing one to image nanometer scale magnetism in real space has been successfully applied to metals like Fe [1] and Mn [2]. However, there is a high interest in probing the nano-magnetism on more complex materials with high potential for spin-valve and magnetic recording applications. A unique candidate in this respect is magnetite (Fe_3O_4) which is a ferrimagnetic stable oxide abundantly found in nature and predicted to be 100% spin-polarized [3], [10], [4]. Thus, the understanding of the structural and magnetic properties of magnetite surfaces down to the atomic scale has attracted considerable research interest. STM investigations on the (110) surface have been performed only with a paramagnetic W tip [5], [11]. Peculiar magnetic properties are expected for the (110) surface, which is predominantly present in the biogenic magnetite crystals [6]. In vertebrates, these crystals are thought to be crucial in magnetoreception, the ability to sense the polarity, the inclination and intensity of the earth's magnetic field and to be involved in navigation.

Magnetite has a face centered cubic inverse spinel crystal structure with a lattice constant of 8.397 Å. The tetrahedral sites are occupied by Fe^{3+} ions and the octahedral sites are shared between equal amounts of Fe^{3+} and Fe^{2+} ions. The two sublattices formed by the octahedral and the tetrahedral sites couple antiferromagnetically and have different magnetic moments resulting in a net magnetization. The conductance takes place at the octahedral sites due to the continuous hopping of electrons between Fe^{2+} and Fe^{3+} ions. Two types of bulk termination exist for the (110) surface: type A contains both tetrahedrally and octahedrally coordinated Fe ions, and type B contains octahedrally coordinated Fe ions [Fig. 3(a)]. The type A and type B layers alternate in the bulk with an interlayer spacing of 1.484 Å. The two types of surface are equally polar [+3 and −3] and thus assuming bulk truncations, the surface is expected to reconstruct.

II. Experiment

The Fe_3O_4 (110) thin films used in this study were deposited on MgO(110) substrates by e-beam evaporation from an Fe wire. The tips used in this study were paramagnetic W tips and antiferromagnetic MnNi tips [7]. The details about the preparation procedure of the tips and samples are presented elsewhere [8]. The samples were inspected by Auger electron spectroscopy (AES) to estimate the degree of contamination in the surface region. The STM/STS measurements were performed at a base pressure below 5×10^{-11} mbar at room temperature with an Omicron UHV STM-1.

III. Results and Discussion

After annealing in UHV at 1000 K, the films showed a well-ordered surface consisting of ridges running along the $[\bar{1}10]$ direction with a 25-Å periodicity corresponding to $p(1 \times 3)$ reconstruction [5], [11]. From the Auger spectra of the annealed films, we derive a contamination level for magnesium of ∼6%. This content of Mg^{2+} ions is sufficient to play an important role in the observed $p(1 \times 3)$ reconstruction. Our STM images acquired with paramagnetic W tips and antiferromagnetic MnNi tips show a surface morphology consisting of terraces with edges perpendicular to the $[\bar{1}10]$ direction. The step heights between terraces are integer multiples of 3.0 Å±0.3 Å. This corresponds to the distance between similar layers (A-A or B-B) in the bulk structure. Each terrace ripples in the $[\bar{1}10]$ direction. The periodicity of the ridges is mostly 25.0 Å±0.3 Å [Fig. 1(a)]. This periodicity corresponds to threefold the bulk lattice constant (8.4 Å). Atomic rows running along the $[\bar{1}10]$ direction [Fig. 1(b)], are often resolved on the tops and in the valleys of our STM images using different W and MnNi tips.

Using a very clean W tip obtained by melting its top through electron bombardment, we observe a significant improvement in the resolution of the STM images. In Fig. 2(b), we show an example of such an image where the top of one ridge with a

Digital Object Identifier 10.1109/TMAG.2006.878405

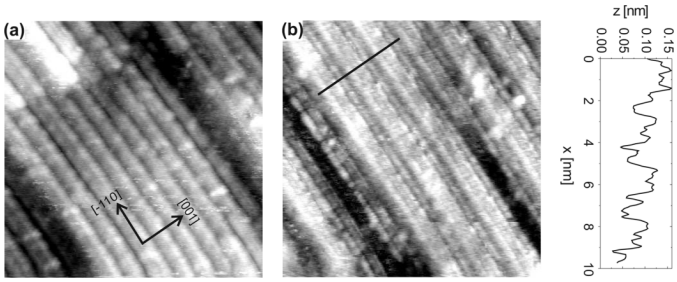

Fig. 1. (a) 350×350 Å^2 STM image taken with a W tip at a set point of $V_S = 1.5$ V, $I = 0.3$ nA and showing ridges along the $[\bar{1}10]$ direction separated by 25 Å. (b) 200×200 Å^2 STM image taken with a W tip at a set point of $V_S = 1.5$ V, $I = 0.28$ nA and showing resolution on tops and valleys of the ridges. A line profile is taken along the [001] direction.

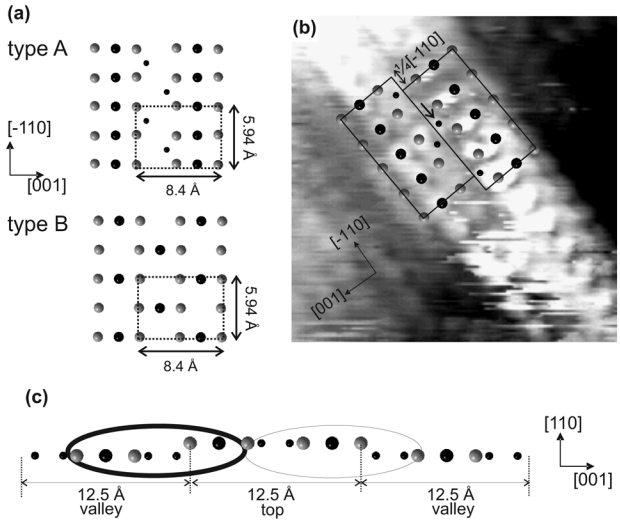

Fig. 2. (a) A and B type (110) layers that alternate in bulk. The surface unit cell is indicated by a rectangle. Large gray, small black, and large black circles denote O, tetrahedral Fe, and octahedral Fe ions, respectively. (b) (30×30) Å^2 atomically resolved STM topography taken with a clean blunt W tip at a set point of $V_S = 1.5$ V, $I = 0.76$ nA and showing periodic features along $[\bar{1}10]$ and [001] directions. On part of the STM topography we indicate atomic positions according to the model based on an A-type bulk layer. The rectangles represent the two sets of atoms that are shifted with a vector of $1/4[\bar{1}10]$ in respect to their bulk positions. The arrow indicates an imaged atom corresponding to the tetrahedral Fe site. (c) The side view of the model projected along the $[\bar{1}10]$ direction. Thick and thin ovals highlight the regions corresponding to the bright and dark regions of the current maps presented in Fig. 3, respectively.

width of 12.5 Å $\pm$ 0.3 Å is very well resolved. This tip images periodicity along both the [001] and $[\bar{1}10]$ directions. The distances between the atoms are in good agreement with the bulk A layer distances. We attribute the indented line on the top of the ridge to the spacing between the tetrahedral Fe^{3+} ions rows of the bulk A layer. The same periods imaged on top of the ridges are identified also in the valleys. The imaged row of atoms in the middle of the valley [observed also in Fig. 1(b)] is attributed to octahedral Fe sites. The very well resolved images taken with blunt W tips allow us to suggest an atomic model of the top region of the ridges. In comparison to a bulk A-type truncation the two sets of atoms highlighted by rectangles in Fig. 2(b) are shifted with respect to each other with a vector of $1/4[\bar{1}10]$. The side view of our structure model projected along the $[\bar{1}10]$ direction is shown in Fig. 2(c). The characteristic period of 25 Å is observed also for a single crystal (110) surface of magnetite

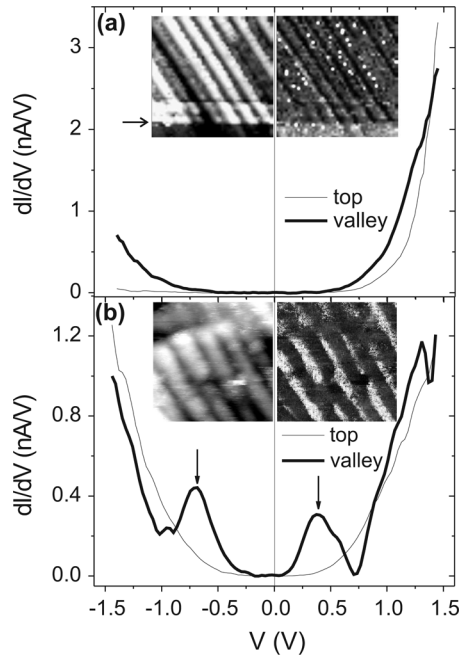

Fig. 3. (a) Derivatives of the *I–V* curves obtained after the change of the W tip state (indicated by an arrow in the left inset) on the tops and the valleys of the ridges. Each curve is the average over approximately hundred single curves. Inset: 200×200 Å^2 STM image taken at a set point of $V_S = 1.5$ V, $I = 1$ nA and corresponding current map at 1.06 V, showing the appearance of a contrast between tops and valleys of ridges when the tip state is changed. (b) Derivatives of the *I–V* curves obtained with a MnNi tip on the tops and the valleys of the ridges. Each curve is the average over approximately hundred single curves. The pronounced features at 0.3 V and -0.7 V present in the valleys are indicated by arrows. Inset: 150×150 Å^2 STM image taken at a set point of $V_S = 1.5$ V, $I = 0.57$ nA and corresponding current map at 0.6 V, showing strong contrast between tops and valleys of ridges.

[5], [11]. Periods in between mesoscopic and atomic often result from a compromise the surface takes between two driving forces: minimization length of magnetic structural boundaries and Coulomb energy.

No sites are visible in our STM images that could be attributed to the Mg^{2+} ions which are present in the surface region as indicated by the Auger analysis. Furthermore the A-type bulk layer has an excess of positive charge and the presence of the Mg^{2+} ions at the outermost layer would increase the surface charge and thus decrease its instability. However, the subsurface layer is of B-type with an excess of negative charge. Thus the Mg^{2+} ions can intercalate at the interstitial positions of octahedral Fe ions rows in the subsurface B layer. This interpretation is in good agreement with the AES measurements.

The conductivity character of the Fe_3O_4 (110) surface is analyzed by means of STS measurements. Semiconductor-like *I–V* curves are preserved down to low tunneling resistances (corresponding to 2-nA tunneling current and 1-V gap voltage). In Fig. 3(a), we present the derivatives of the *I–V* curves measured on top and in the valleys of the ridges of the topography image shown in the left inset of Fig. 3(a). The current map at 1.06-V bias voltage is presented in the right inset of Fig. 3(a). The STS data presented in this figure is the third one from a sequence of four consecutive STS measurements performed in the area presented in Fig. 1(b). For the first two measurements the top-valley corrugation in the topography was $\sim$1 Å and very small contrast

has been observed in the corresponding current map. The same situation is observed for a part [below the arrow in Fig. 3(a)] of the third measurement. At one point (the part of the image above the arrow in Fig. 3(a)) the state of the tip has changed resulting in an increase in top-valley corrugation to $\sim$3 Å and a contrast in the current map associated with the ripple structure. This situation is maintained also for the fourth measurement. By superimposing the current map on the topography image, a slight shift is observed, such that the brighter zones (higher conductance) in the current map correspond to the main part of the valley and a small part of the top in topography, while the darker zones (lower conductance) correspond to the main part of the tops and a small part of the valleys. In the structure model presented in Fig. 2(c) we highlight the regions corresponding to the bright and dark regions in the current map, by the thick and thin ovals, respectively. For practical reasons, these regions will be referred in the following as corresponding to valleys and tops of the ridges.

The STS measurements performed with an antiferromagnetic MnNi tip show large differences between the conductivity in the valleys and the conductivity on the tops of the ridges with two pronounced features at 0.3 V and -0.7-V bias voltages [indicated by arrows in Fig. 3(b)]. Fig. 3(b) shows the *dI/dV* curves measured in the valleys and on the tops of the ridges. The STM image and the corresponding current map at 0.6 V bias voltage are presented in the inset of Fig. 3(b). The strong dark-bright contrast correlates to the ridge structure in the same manner as the contrast measured with the W tips. The two pronounced features at 0.3 V and -0.7 V are present only in the valleys and have never been observed in the *dI/dV* curves in the measurements performed with W tips at different set points ($V_S = 1.5$ V and $I = 0.1\ \mathrm{nA} \div 1$ nA). Although less pronounced, a different MnNi tip shows similar features at 0.3 V and -0.7 V, strengthening the validity of these results.

According to the model presented in Fig. 2(c), the top of the ridges are dominated by the tetrahedral contribution, while the valleys are dominated by the octahedral contribution. This explains the small contrast typically observed in the current maps acquired with W tips. Furthermore, as the octahedral sites are responsible for the conduction mechanism in magnetite, the always measured higher conductance in the valleys agrees with the dominant octahedral character of our model. In magnetite, the octahedral and the tetrahedral sublattices have antiparallel orientations of the magnetic moments. Based on our proposed model, the octahedral character of the valleys and the tetrahedral character of the tops result in an antiparallel orientation of the magnetization vectors on tops and valleys. When using a magnetic tip, the detection of the spin polarization component results in an enhanced contrast in the current map and an enhanced corrugation in the topography between tops and valleys due to their antiparallel oriented magnetization directions.

A plausible explanation for the change of the W tip state [see arrow Fig. 3(a)] refers to a soft crash of the tip during the STS measurements when the tip picked up material from the film. Thus, hereby the tip is rendered spin selective to certain degree. The detection of the spin polarized contribution to the tunneling current leads to a corrugation enhancement and a stronger appearance of the top-valley contrast in the current map, as observed above the arrow in Fig. 3(a).

The MnNi tip shows a strong bright-dark contrast in the current map that we attribute to magnetism. Surprisingly, the features at 0.3 V and -0.7 V observed with the MnNi tips are present only in the valleys and have never been observed in the *dI/dV* curves measured with a W tip. We believe that these features are surface states stemming from octahedral Fe. This is much more probable than being due to tip electronic states, as they are not observed in the valleys, neither on Mn films grown on Fe(001) measured with MnNi tips [9]. However, although less pronounced, they should be visible also with spin-integrated tips, i.e., W tips. Thus, at the moment, we cannot exclude the contribution of the tip density of states that can lead to emphasis or suppression of features, e.g., magnetochemistry.

IV. Conclusion

The STM study on a Fe_3O_4 (110) surface indicates a morphology consisting of terraces that ripple in the $[\bar{1}10]$ direction. Atomically resolved images allows us to build a model that explains the weak contrast between tops and valleys observed in the current maps acquired with W tips. Our STS data obtained with an antiferromaganetic MnNi tip show unexpected spectroscopic features, associated with octahedral magnetic sublattice (valleys). Thus, magnetic and structural domains correlate.

Acknowledgment

This work was supported in part by the ASPRINT European project (NMP-CT-2003-001601), Nanomed, the Dutch nanotechnology program of the Ministry of Economic Affairs, and The Netherlands Foundation for Fundamental Research on Matter (FOM).

References

[1] A. Kubetzka, P. Ferriani, M. Bode, S. Heinze, G. Bihlmayer, K. von Bergmann, O. Pietzch, S. Blügel, and R. Wiesendanger, *Phys. Rev. Lett.*, vol. 94, 2005. 087204.
[2] T. K. Yamada, M. M. J. Bischoff, G. M. M. Heijnen, T. Mizoguchi, and H. van Kempen, *Phys. Rev. Lett.*, vol. 90, 2003. 056803.
[3] A. Yanase and N. Hamada, *J. Phys. Soc. Jpn.*, vol. 53, p. 312, 1984.
[4] Z. Zhang and S. Satphaty, *Phys. Rev. B*, vol. 44, 1991. 13319.
[5] R. Jansen, V. A. M. Brabers, and H. van Kempen, *Surf. Sci.*, vol. 328, p. 237, 1995.
[6] D. A. Bazylinski and R. B. Frankel, *Nat. Rev., Microbiol.*, vol. 2, p. 217, 2004.
[7] S. F. Ceballos, G. Mariotto, S. Murphy, and I. V. Shvets, *Surf. Sci.*, vol. 523, p. 131, 2003.
[8] G. Maris, L. Jdira, J. G. H. Hemrsen, S. Murphy, G. Manai, I. V. Shvets, and S. Speller, *J. Phys. Soc. Jpn.*, vol. 45, p. 3B, 2006.
[9] T. K. Yamada, Ph.D. dissertation, Radboud Uiversity Nijmegen, The Netherlands, 2004.
[10] A. Yanase and N. Hamada, *J. Phys. Soc. Jpn.*, vol. 68, p. 1607, 1999.
[11] R. Jansen, R. M. Wolf, and H. van Kempen, *J. Vac. Sci. Technol. B*, vol. 14, p. 1173, 1996.

Manuscript received March 10, 2006 (e-mail: g.maris@science.ru.nl).